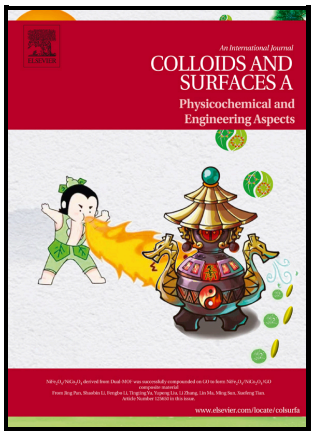
Journal Pre-proof

TiO_2-enhanced Chitosan/Cassava Starch Biofilms For Sustainable Food Packaging



Francisco Leonardo Gomes de Menezes, Ricardo Henrique de Lima Leite, Francisco Klebson Gomes dos Santos, Adrianus Indrat Aria, Edna Maria Mendes Aroucha

PII: S0927-7757(21)01530-2

DOI: https://doi.org/10.1016/j.colsurfa.2021.127661

Reference: COLSUA127661

To appear in: *Colloids and Surfaces A: Physicochemical and Engineering Aspects*

Received date: 24 July 2021
Revised date: 28 September 2021
Accepted date: 29 September 2021

Please cite this article as: Francisco Leonardo Gomes de Menezes, Ricardo Henrique de Lima Leite, Francisco Klebson Gomes dos Santos, Adrianus Indrat Aria and Edna Maria Mendes Aroucha, TiO_2-enhanced Chitosan/Cassava Starch Biofilms For Sustainable Food Packaging, *Colloids and Surfaces A: Physicochemical and Engineering Aspects,* (2021) doi:https://doi.org/10.1016/j.colsurfa.2021.127661

This is a PDF file of an article that has undergone enhancements after acceptance, such as the addition of a cover page and metadata, and formatting for readability, but it is not yet the definitive version of record. This version will undergo additional copyediting, typesetting and review before it is published in its final form, but we are providing this version to give early visibility of the article. Please note that, during the production process, errors may be discovered which could affect the content, and all legal disclaimers that apply to the journal pertain.

© 2021 Published by Elsevier.

Colloids and Surfaces A: Physicochemical and Engineering Aspects, Volume 630, December 2021, Article number127661
DOI:10.1016/j.colsurfa.2021.127661
Journal Pre-proof

TiO_2-enhanced chitosan/cassava starch biofilms for sustainable food packaging

Francisco Leonardo Gomes de Menezes[a1], Ricardo Henrique de Lima Leite[b], Francisco Klebson Gomes dos Santos[c], Adrianus Indrat Aria[d2], Edna Maria Mendes Aroucha[e3]

a Universidade Federal Rural do Semi-Arido, Brazil, leonardoquimico@ufersa.edu.br;
b Universidade Federal Rural do Semi-Arido, Brazil, ricardoleite@ufersa.edu.br;
c Universidade Federal Rural do Semi-Arido, Brazil, klebson@ufersa.edu.br;
d Surface Engineering and Precision Centre, Cranfield University, United Kingdom, a.i.aria@cranfield.ac.uk;
e Universidade Federal Rural do Semi-Arido, Brazil, aroucha@ufersa.edu.br;

ABSTRACT

Biopolymeric films with the addition of nanoparticles have been studied as an alternative to replace petroleum-based synthetic packaging, which is difficult to recycle and leads to a major environmental problem. The goal of this study is to develop and characterise biopolymeric films of chitosan and cassava starch with the addition of titanium dioxide (TiO_2) nanoparticles for use as food packaging. Chitosan film (2% w/w), cassava starch film (2% w/w), and chitosan/cassava starch (1:1) blend were developed in the absence and presence of TiO_2 nanoparticles (0.25 and 1% w/w) and characterised in terms of physicochemical properties. The results indicate that the properties of films related to water (permeability, solubility, and water sorption) and mechanical (tension, elongation, and Young's modulus) are strongly influenced by the characteristics of the biopolymers used and can be improved with the introduction of TiO_2. The water sorption was reduced with the addition of TiO_2, which makes the film more hydrophobic and exhibits a higher tensile strength by more than 15% and elongation by more than 100%. The addition of 1% TiO_2 also leads to a reduction in transmittance of 97% in UVA, UVB, and UVC regions, which is a valuable feature for food preservation.

Keywords: Bionanocomposite; Biopolymers; Titanium Dioxide; Cassava Starch; Chitosan.

Corresponding authors:
[1] Francisco Leonardo Gomes de Menezes. E-mail: Address: Av. Francisco Mota, 572 - Bairro Costa e Silva, Mossoró RN/CEP: 59.625-900, +55 84 3317-8200, leonardoquimico@ufersa.edu.br.
[2] Adrianus Indrat Aria. E-mail: a.i.aria@cranfield.ac.uk.
[3] Edna Maria Mendes Aroucha. E-mail: aroucha@ufersa.edu.br.

Published by Elsevier. This is the Author Accepted Manuscript issued with: Creative Commons Attribution Non-Commercial No Derivatives License (CC:BY:NC:ND 4.0).
The final published version (version of record) is available online at DOI:10.1016/j.colsurfa.2021.127661. Please refer to any applicable publisher terms of use.

1. Introduction

Food packaging is a fundamental element of food preservation. It protects food from external microbial and environmental influences and contributes to the preservation of food organoleptic and nutritional quality. Despite their excellent performance and durability, non-biodegradable petrochemical polymeric materials have introduced a significant ecological problem due to their energy-intensive recycling process and long degradation in the environment. Biopolymers are promising alternatives, as they exhibit low toxicity, can be degraded biologically, and are environmentally friendly [1–3] The biophysical and mechanochemical properties of biopolymers are highly tailorable based on their origin, chemical structures, applied treatments, additives, and composition in the mixtures, making them versatile for use in a wide variety of applications [4–8]. Thin films of biopolymers, known as biofilms, have recently emerged as a viable option for food packaging or coating to allow safe storage and transportation of food [4,9].

Amongst a wide range of biodegradable biopolymers, chitosan and starch are of particular interest, as they are abundant, inexpensive, and can form films and coatings for food preservation [10]. Chitosan, the second most abundant natural biopolymer after cellulose, is a natural antimicrobial polysaccharide-amino acid complex obtained mainly through the process of deacetylation of chitin from crustacean shells [3,11,12]. Starch is a non-toxic, low-cost, stable, and gel-forming polysaccharide that has been widely used as the main constituent of edible coatings. The combination of these properties makes chitosan/cassava starch biofilms a strong contender in the development of eco-friendly food-preserving coatings and packaging [13]. Nonetheless, like most biopolymers, these blends are still relatively hydrophilic, such that their mechanical stability, water resistance, and moisture barrier capabilities are still far from ideal [10,14,15]. To overcome these shortcomings, many studies seek to improve the biofilm properties and thus food-preserving performance by incorporation of nanoparticles in a form of bionanocomposites [8]. Many previous studies have reported the development of bionanocomposite films based on potato, cassava starch and chitosan reinforced with cellulose nanofiber [12], potato starch /TiO_2 [16], wheat starch/TiO_2 [17], *Iberian Lallemantia* mucilage/TiO_2 [18], chitosan/TiO_2 [19], zein/chitosan/TiO_2 [20], hydroxypropyl methylcellulose/TiO_2 and gelatin/TiO_2 [21], and chitosan/TiO_2 to prolong the storage life of tomato [22] and mango fruits [23].

Nanoparticulate metal oxides-based food additives have been at the forefront of the search for better functional properties of biopolymeric films. Titanium dioxide (TiO_2) nanoparticles are one of these metal oxides that have been frequently used as food additives, known as E171, to improve the texture, colour, longevity, and aesthetics of food [22,24,25]. TiO_2 nanoparticles are UV absorbing materials with good dispersion properties, fast electron transfer rate, antimicrobial

activities, and can interact with the polar groups of biopolymer matrices to enable economical bionanocomposites with improved characteristics [16–18]. TiO_2 nanoparticles are also an excellent alternative to traditional UV blocking agents in food packaging to prevent detrimental effects on foods, such as breakdown of vitamins and proteins, changes in colours and flavours, degradation of antioxidants, and oxidation of lipid [26]. The capabilities of TiO_2 nanoparticles to produce reactive oxygen species by absorbing photoenergy in the UV-Visible wavelength range are highly sought after in food preservation, as they actively contribute to the inactivation of bacteria and fungi that cause food spoilage [22,23,27].

In recent years, several studies have been carried out to explore the prospect of modifying the physicochemical properties of various biopolymer matrices through TiO_2 nanoparticles incorporation for use in food packaging materials [16–20,22,23,26,28]. To date, however, there is a knowledge gap in the development of TiO_2-enhanced bionanocomposites, particularly on chitosan-cassava starch biopolymeric matrices for use in biodegradable food packaging. Considering this unprecedented work and the notable importance of obtaining a sustainable and ecologically friendly solution for use in the growing global food industry and the ever-pressing challenges with food waste, it is timely and critical to further advance the understanding of the influence of TiO_2 nanoparticles on the properties of chitosan-cassava starch biofilms. In this study, we systematically investigate the effect of two different concentrations of TiO_2 nanoparticles on the mechanical properties, water interaction, optical characteristics of chitosan-cassava starch biofilms. We report herein the incorporation of TiO_2 nanoparticles to enable improvement in tensile strength, hydrophobicity, and UV transmittance of chitosan-cassava starch bionanocomposite films.

2. Materials and methods

2.1.Materials

The materials used in this study are chitosan (M_W 50000 Da, deacetylation degree ≥ 88.91% Polymar Indústria e Com. Imp. e Exp. Ltda - Brazil), cassava starch [29.24 % (± 0.68) amylose and 70.76% (± 0.68) amylopectin] (Indústria Primícia do Brazil Ltda - Brazil), acetic acid (99.7%, purity, Dinâmica Química Contemporânea Ltda - Brazil), glycerol (99.5% purity, Dinâmica Química Contemporânea Ltda - Brazil), and TiO_2 nanoparticles (anatase, particle size of 20-25 nm, 99.7% purity, Sigma-Aldrich).

2.2.Synthesis of chitosan/cassava starch/TiO_2 bionanocomposite films

Filmogenic solutions forming 2% w/w chitosan film (CH) and 2% w/w cassava starch film (ST) were prepared using methodologies adapted from previous studies [7,29]. CH was prepared by adding 2% w/w of chitosan powder in a 1% w/w acetic acid solution and stirred for 24 hours to complete dissolution using a magnetic stirrer. ST was prepared by dispersing Cassava starch powder in distilled water at 70 ± 5 °C for 30 min under constant agitation to complete the gelatinization process. To obtain the film-forming solutions for the blend of chitosan 1% w/w + cassava starch 1% w/w (CH/ST), the abovementioned CH and ST solutions are mixed with a ratio of 1:1 while keeping the total dry mass constant. Glycerol was used as a plasticizer at a concentration of 20% w/w in relation to the dry mass of biopolymer. Bionanocomposites were prepared by adding TiO_2 nanoparticles in concentrations of 0.25 and 1% (w/w) in relation to the dry mass of the biopolymeric mixture of cassava starch, chitosan, and glycerol.

Previous studies show that the incorporation above 1% of TiO_2 favours the formation of aggregates [19,21,30], which justifies the optimization of concentrations of 0.25 and 1% of TiO_2 in our study to obtain nanocomposites with improved properties. Suspension of TiO_2 nanoparticles at a concentration of 0.25 and 1% were added slowly (1mL min^{-1}) with stirring (1000 rpm) over 5 min into the CH / ST filmogenic solution (CH / ST / T0.25%, CH / ST / T1% respectively). They were then cooled to room temperature (23 °C) and sonicated in an ultrasound bath (Quimis, Q3350) for 10 min with frequency and ultrasonic power of 40 KHz and 135 watts RMS, respectively. Subsequently, 60g of the solution were deposited on 15 cm wide, 15 cm long, and 2 cm deep acrylic plates and dried by evaporating the solvents in an air circulation oven for 4–6 hours, as has been described in detail elsewhere [7]. All films were stored at 23 °C and 55% relative humidity. Figure 1 shows schematic representation of the film preparation and synthesis.

2.3. Bionanocomposite films characterisation

The film thickness was determined by a digital micrometre (Mitutoyo MDC-25M, MFG-Japan) in 5 different positions and the obtained results were then averaged. The methodology for solubility measurement was adapted from a previous study [7], where the initial mass of the films was obtained by drying the films at 105 °C for 1 hour. The final mass was obtained by immersing the films in distilled water under agitation for 24 hours at 23°C and then dried under the same conditions. Solubility in water was calculated using Eq. (1):

$$S = (m_i - m_f / m_i)\text{x}100 \quad (1)$$

where S is the water solubility in %, m_i is the initial mass of the film in g, and m_f is the final mass of the film in *g*.

Water vapour permeability was determined using a gravimetric method (ASTM E96 / E96M-12), where the films were sealed in cells containing 6 mL of water. Each film was initially weighed and placed in silica-containing desiccators with a relative humidity of 50% and an internal temperature of 23 °C. Periodic weighing of each cell was carried out at intervals of 1 hour for a total of 8 hours. Water vapour permeability was obtained using Eq. (2):

$$\mathrm{WVP} = W.L/A.t.\Delta P \quad (2)$$

where WVP is the Water Vapour Permeability in g.mm/h.kPa.m^2, W is the weight of the water that permeates across the film in g, L is the average film thickness in mm, A is the exposed area in m^2, t is the permeation time in h, and ΔP is the water vapour pressure differential across the film in kPa.

Tensile strength, elongation at break, and modulus of elasticity were assessed by a tensile test using a universal testing machine (DL5000/10000 Series Instron EMIC 23) under ASTM D882-83 method at a displacement rate of 5mm.min^{-1}. Each test specimen was 50 cm long, 5 mm wide, and about 0.07 mm thick. The absorbance spectra of the films were measured using a UV-vis spectrophotometer (EVO-600PC, Thermo Scientific). Each test film was cut and placed in a test cell with a blank cell without film as the reference. The transmittance was obtained through the Beer-Lambert law and the opacity of the films was then calculated by Eq. (3).

$$\mathrm{Op} = Abs_{600}/X \quad (3)$$

where Op is the opacity in AU.Nm.mm-1), Abs600 is the absorbance at a wavelength of 600 nm, and X is the film thickness in mm.

Colorimetric analysis was performed by reflectometry with a portable colorimeter (Konica Minolta Sensing Inc. Japan) using a methodology adapted from previous studies [16,18]. A standard black plate was used (L* = 1, a* = 0 and b* = 0) as the background for the films. Luminosity (L) ranges from 0 (dark/opaque) to 100 (white), a represents green (negative) and red (positive), while b represents blue (negative) and yellow (positive). Equidistant points in the films were measured and the readings were averaged. The total color difference (ΔE), whiteness (WI), and yellow (YI) indices of the samples were calculated using Eq. (4–6), respectively.

$$\Delta E = \sqrt{(L^* - L)^2 + (a^* - a)^2 + (b^* - b)^2} \quad (4)$$

$$WI = 100 - \sqrt{(100 - L)^2 + a^2 + b^2} \quad (5)$$

$$YI = 142.86b/L \quad (6)$$

The film morphology was evaluated under high magnification imaging with a scanning electron microscope (TESCAN VEGA 3). The samples were sputter-coated with a few nm of Au (Quorum Tech Q150R) prior to the microscopy. The film surfaces were imaged by applying an acceleration voltage of 10 kV with a magnification of 5 kx, while the fractured cross-sections were imaged with 5 kv acceleration voltage and 500x magnification. The crystalline phases of the films were analysed using an X-ray diffractometer (Shimadzu, XRC-6000) in a 2θ range of 10°–60°, with a source of Cu Kα radiation at a wavelength of 0.15 nm. Diffractograms were obtained using a voltage of 40 kV, a current of 40 mA, and a sweep rate of 2 min^{-1}. The amorphous and crystalline areas in diffractograms were analysed by deconvolution using OriginPro8 software.

The film behaviour under different relative humidity environments was investigated using water sorption isotherms measurements with the Guggenheim-Anderson and Boer (GAB) model. The water sorption measurements were adapted according to the method described in a previous study [18]. Biopolymer films with dimensions of 30 mm x 30 mm were placed in separate silica gel (10%) containing hermetically-sealed plastic containers with supersaturated saline solutions at a relative humidity (UReq) range of 10–97%. The supersaturated saline solutions used here were comprised of CH_3COOK (23%), $CaCl_2$ (27%), $MgCl_2.6H_2O$ (33%), K_2CO_3 (44%), Mg $(NO_3)^2$ (55%), KI (68.9%), NaCl (75%), KCl (85%), K_2CrO_4 (88%), and K_2SO_4 (97%). The water activity values (a_w = UReq / 100) were calculated for a temperature of 23 °C and the films were weighed at 24 hours intervals. They were then dried in an oven at 105 ± 2 ºC to determine the dry mass of the samples. Water content was calculated by subtracting the dry weight from the sample weight prior to drying. The water sorption isotherms obtained were calculated using GAB model Eq. (7).

$$X = x_m c k a_w / (1 - k a_w)(1 - k a_w + c k a_w) \quad (7)$$

where X is equilibrium water content (g water / g dry matter), x_m is the water content in the monolayer (g water / g dry matter), a_w is the water activity, c indicates binding energy of sorption, and k indicates the degree of freedom of water.

2.4 Statistical analysis

The experiment was randomized with five treatments and five repetitions (5 x 5), and the means were compared using the Tukey test at 5% significance level. The data of the sorption isotherms were adjusted using non-linear regression. The values of determination coefficients (R^2) were calculated and used to evaluate the adjustment of the GAB model to experimental data.

3. Result and discussion

3.1. Morphological analysis

Figure 2 shows SEM images of the surface and cross-section of the mechanically cleaved edge in the biofilms of chitosan (CH), cassava starch (ST), chitosan/cassava blend (CH/ST), and the bionanocomposites with TiO_2 concentrations of 0.25% and 1% (CH/ST/T0.25% and CH/ST/T1%). CH films show a homogeneous surface, which is more homogeneous compared to the other films, and the fracture section shows the presence of dense exfoliations with ductile fracture behaviour. ST films show a heterogeneous surface with higher roughness and the fracture section exhibit cracks that indicate brittle fracture behaviour. ST contains a mixture of amylose and amylopectin with a great number of hydrophilic groups that can interact with water and thus higher mobility when wet. However, ST appears to be relatively brittle when dry. CH/ST blends show intermediate characteristics on the surface and in the fracture section, with a reduction of cracks indicating a more ductile fracture. This suggests that the interaction of different polymeric chains in the biopolymeric CH/ST blends leads to better mechanical properties that do not occur when each of the polymers is in isolation.

The addition of TiO_2 nanoparticles to the CH/ST blend changes the surface morphology of the films. CH/ST/T0.25% shows many agglomerated TiO_2 nanoparticles in the polymer matrix and the fracture section shows small voids perpendicular to the rupture of the film. Anatase TiO_2 nanoparticles are known to be easily agglomerated in mild acidic range of $5 < pH < 7$ due to their surface charge neutralisation [31,32] These agglomerates have the tendency to further grow in size above certain critical radius and form micron-size networks, hence easily observable by SEM (Figure 2d), by solvent evaporation process during the film fabrication step [33,34]. Note that the biopolymeric blends are mildly acidic from the use of 1% w/w acetic acid to initiate the dissolution of CH. It is postulated herein that intermolecular forces are formed between TiO_2 nanoparticles and the hydrophilic -OH and $-NH_2$ groups from starch and chitosan, respectively [22,35]. However, the

poor distribution of low concentration of inorganic TiO_2 nanoparticles (0.25% w/w) in the biopolymeric blends of organic CH/ST (1:1) matrix suggests that their interactions are relatively weak.

The increase in TiO_2 concentration to 1% results in more homogeneous surface morphology with few apparent agglomerations. The fracture section of CH/ST/T1% shows a more compacted matrix with small clusters. This finding is slightly counterintuitive, as one would expect further agglomeration with a higher concentration of TiO_2 nanoparticles. However, previous study suggests that the abundance of TiO_2 nanoparticles improves the relatively weak interaction between the Lewis sites of TiO_2 with the -NH2 groups from the chitosan [35]. The improved polymer-particle interactions through primary and secondary bonds increases the repulsive interaction potential and aggregation barrier, and thus reduces the agglomeration tendencies of TiO_2 in the CH/ST matrix [36]. This observation agrees with the previous study [19], where the incorporation of 1% of TiO_2 in chitosan films results in homogeneous films with improved properties, above which agglomeration of the nanoparticles is likely to reoccur. In agreement with this previous study, the maximum concentration of TiO_2 in biopolymer blends is constrained at 1% herein to avoid excessive agglomeration. Such a homogeneous and ordered distribution of TiO_2 nanoparticles in CH/ST/T1% is expected to result in a modification of the film properties.

3.2. Crystalline phase analysis

The XRD patterns of CH, ST, CH/ST, CH/ST/T0.25%, and CH/ST/T1%, along with that of pure TiO_2 nanoparticles are shown in Figure 3. As confirmed by XRD, the TiO_2 nanoparticles used in this study are mainly in anatase form with a small percentage of rutile as an impurity [19]. CH shows a prominent peak at 2θ of ~20° that can be attributed to the (110) plane of deacetylated α-chitosan, which is consistent with existing literature [19, 37–39] who reported the highest peak of crystallinity pure chitosan could be observed at 20.40º, 20.38º and 19.7º respectively. ST shows a much broader peak at 2θ of 17–20° that suggests a less crystalline structure than that of CH. The relative crystallinities were calculated to be ~17% and ~16% for CH and ST, respectively. As shown by CH/ST, the blend of CH and ST results in a shifted peak at 2θ of ~19° with relative crystallinity of 14%. The addition of TiO_2 nanoparticles to the blend shows distinctive TiO_2 diffraction peaks that can be easily recognised in the spectra of CH/ST/T0.25% and CH/ST/T1% films. These peaks become more pronounced with the increase in TiO_2 content and peaks attributed to crystalline TiO_2 can be easily observed in the CH/ST/T1%. The relative crystallinities were

calculated to be ~12% and ~17% for CH/ST/T0.25% and CH/ST/T1% films, respectively. As a comparison, the relative crystallinity of TiO_2 nanoparticles was calculated to be ~68%.

3.3. Water vapour permeability – WVP

Figure 4 shows water vapour permeability (WVP) for biopolymers without TiO_2 (CH, ST, and CH/ST) and bionanocomposites with TiO_2 (CH/ST/T0.25%, and CH/ST/T1%). ST exhibits the lowest WVP at 9.5746 ± 0.3122 g.mm/h.kPa.m², while CH presents the highest WVP at 20.7380 ± 1.5643 g.mm/h.kPa.m². As expected, WVP of CH/ST is somewhere between that of CH and ST at 14.5608 ± 1.4807 g.mm/h.kPa.m². The addition of TiO_2 nanoparticles slightly reduces the WVP, although this is not significant ($p < 0.05$). Nonetheless, the addition of TiO_2 nanoparticles sufficiently reduces WVP to the point of making it statistically equal ($p < 0.05$) to ST, which has the lowest WVP obtained in this study. This reduction in WVP suggests that TiO_2 inhibits the diffusion of water vapour through the film. An interaction of TiO_2 with the hydrophilic groups -OH and $-NH_2$ within the films can also occur, decreasing the availability of the hydrophilic groups and reducing water interactions with the film [16,18,19,22,35,40].

3.4. Solubility in water

Figure 5 shows water solubility for CH, ST, CH/ST, CH/ST/T0.25%, and CH/ST/T1%. The solubility for CH, ST, and CH/ST films were 19.2760 ± 2.0364, 49.7072 ± 1.7766, and 18.6481 ± 1.2091, respectively. This strongly suggests that chitosan content is a key determining factor in reducing the water solubility of the films. Adding chitosan to cassava starch reduced the water solubility by more than 62%. Note that starch by itself has the disadvantage of having high hydrophilicity. The introduction of chitosan leads to the formation of a chitosan/starch blend with reduced hydrophilic -OH groups due to the interactions between functional NH_3^+ groups from the protonated chitosan and OH^- groups from the starch. The reduction in hydrophilic groups ultimately results in a more hydrophobic film [41,42].

The addition of TiO_2 leads to a slight reduction in solubility, although such a reduction is not significant ($p < 0.05$). However, the addition of 1% of TiO_2 is sufficient to reduce the solubility to the point of making it statistically smaller ($p < 0.05$) than either CH by 23% or ST by 70%. This suggests that the TiO_2 nanoparticles interacted by hydrogen bonds with the remaining hydrophilic groups in the biopolymeric blend, leading to more hydrophobic nanocomposites. [18,30]. This result is consistent with studies by Fonseca *et al*. (2020) [21], where a reduction in the solubility of

the Gelatin-TiO_2 nanocomposites was observed from 69.13 ± 4.75 to 45.83 ± 0.94 (%) with the addition of 1% of TiO_2 and the previous study with kefiran-whey-protein-isolate and potato starch [16,43].

3.5. Mechanical properties

Figure 6 shows variations in tensile strength, elongation at break, and Young's modulus of the bionanocomposites. CH exhibits the highest tensile strength at 54.3045 ± 2.8686 MPa, while ST exhibits the lowest at 29.3046 ± 1.1396 MPa (Figure 6a). This can be related to the aforementioned XRD analysis (Figure 3), where CH is a semicrystalline biopolymer and ST is less crystalline than CH. It is expected that CH/ST blends show an intermediate tensile strength at 43.8784 ± 2.5346 MPa, which is about 49% higher than that of ST. It is important to note that the presence of TiO_2 influences the tensile strength in both ways. Tensile strength significantly decreases ($p < 0.05$) when 0.25% of TiO_2 was added (CH/ST/T0.25%), while the addition of 1% of TiO_2 (CH/ST/T1%) leads to a significant increase ($p < 0.05$) by 15% (Figure 6a). This may be due to the heterogeneous TiO_2 dispersion in the polymeric matrices at 0.25%, as evidenced in the morphological analysis (Figure 2). As shown by the irregularities in the fracture section, such heterogeneity may have acted as stress concentrators that weaken the mechanical properties of CH/ST/T0.25%. In contrast, the higher tensile strength of CH/ST/T1% can be attributed to a homogeneous dispersion of TiO_2 in the biopolymeric matrices.

For biopolymer films without TiO_2, the CH/ST blend is found to be significantly ($p < 0.05$) higher than individual CH and ST films. The incorporation of 0.25 and 1% TiO_2 into the blend increases the elongation at the fracture point by more than 85% and 100%, respectively (Figure 6b). CH/ST/T0.25% exhibit Young's modulus of 955.2863 ± 63.5443 MPa, while that of CH/ST/T1% is found at 440.4433 ± 60.2287 MPa. Note that the increase in TiO_2 concentration leads to a significant decrease in the stiffness ($p < 0.05$), as reflected by an increase in elongation at break and a decrease in Young's modulus while improving the tensile strength (Figure 6a). This strongly suggests that the incorporation of TiO_2 nanoparticles in adequate amounts may indeed lead to improvements in mechanical properties through electrostatic interactions and hydrogen bonds. This finding is aligned with previous studies on wheat starch [17], gelatin [44], and whey protein [45].

Journal Pre-proof

3.6. Water sorption isotherms

Figure 7 shows the water sorption experimental observation and the respective fitted GAB model isotherms for CH, ST, CH/ST, CH/ST/T0.25%, and CH/ST/T1% films at 25 °C. Experimental data show the sigmoidal behaviour of an increase in the amount of water per dry matter (X) as water activity (a_w) increases. The water sorption of the films shows a characteristic behaviour that shows changes in the polymeric matrix due to the interaction of water molecules and the hydrophilic groups of the polymers [18,46–51]. A small increase in X at a low water activity (a_w <0.2) can be attributed to the interaction of water in the polymer monolayer. An increase in X at an intermediate water activity (0.2 <a_w <0.75) is related to the interaction of water with hydrophilic groups in the upper layers of polymers. A more significant increase in X at a higher water activity (a_w > 0.75) is mostly due to water condensation in the biopolymer and subsequent dissolution of materials.

The observed behaviour can be considered as type II water sorption isotherm [49] and is analogous to hydrophilic materials [50,52]. X is found to be higher in CH and ST across a wide range of a_w than in CH/ST blends. This suggests that the interactions of polar groups with water are greater in separate biopolymers than in the polymer mixture. In the case of polymer mixture, the interactions that occur between polar groups of different polymer chains suppress its ability to interact with water molecules. Polymers with hydrophilic nature such as chitosan and cassava starch are often mixed to improve their properties [42]. The increase in the concentration of TiO_2 nanoparticles leads to a reduction in water adsorption that indicates greater water resistance. The interaction of TiO_2 with the remaining hydrophilic groups of the polymer effectively reduces further the number of interactions available for water molecules, which results in a less hygroscopic matrix. Such behaviour has been observed in other polymeric matrices [18,48,49] where the increase of TiO_2 concentration leads to a lower equilibrium X over a wide range of a_w. The Guggenheim-Anderson and Boer (GAB) model can be applied to a wide range of a_w and is widely used to describe water sorption phenomena in food products [49]. Table 1 shows the calculated constants for the GAB model.

As observed in previous studies, the R^2 values show a good fit of the GAB model to experimental data (Table 1) [18,48–50]. The adjusted GAB model provides an approximation of X_m, which indicates the largest amount of water per dry material that can be fixed in just a single layer [53]. The highest value for X_m is exhibited by ST film at 0.7047 g/g. X_m is reduced with the introduction of chitosan to the CH/ST blend (0.4662 g/g) and is further reduced with the increase of TiO_2 concentration in the blend. This strongly suggests the importance of the blend formation and

addition of TiO_2 nanoparticles to increase the hydrophobicity of biopolymer films. This finding is in agreement with the previous work on mucilage films of *Iberian Lallemantia* and chitosan/whey protein blend [18,49] that shows a reduction of X_m when TiO_2 is added into the films.

The fitting parameter C represents the binding energy of sorption [54], where a low value of C corresponds to weakly adsorbed water molecules on the biopolymer surface and consequently have a high degree of freedom. The fitting parameter K indicates the degree of freedom of water molecules in the adsorbent multilayer. K is important as it provides information on whether water is adsorbed as a multilayer or a free state. For K close to 1.0, the difference between multilayer sorption energy and water condensation energy is small, and thus the multilayer may have the properties of liquid water. The lowest K is observed on bionanocomposite films containing the highest concentration of TiO_2 (CH/ST/T 1%) with a value of 0.5914. This result is consistent with the aforementioned solubility (Figure 5) and mechanical properties (Figure 6) of the bionanocomposite films, which suggests a significant decrease in the number of polar groups available for interactions with water molecules once various interactions between the polymer mixture with the added TiO_2 nanoparticles have been formed.

3.7. Thickness and colour parameters

Table 2 shows the thickness and colour parameters of the biopolymer films. Many factors may influence the film colour, including the crystallinity and size of TiO_2 nanoparticles, the film thickness, and the film preparation and manufacturing processes [17]. The incorporation of TiO_2 nanoparticles does not significantly influence ($p < 0.05$) the thickness of the films, which have an average thickness value of 0.057 nm, in alignment with previous studies [18,26]. The colour parameters are found to be highly dependent on the type of biopolymer used, the interaction between constituent biopolymers in the blends, and the content of TiO_2. Regarding the films without TiO_2, the values of lightness (L), colour difference (ΔE), and whiteness index (WI) for CH are higher than those of ST and CH/ST blends. Note that the cassava starch powder used for the manufacture of ST films was white while the chitosan powder for CH films was yellow. However, the obtained ST films are observed to be colourless with a WI of 30.23. Similar behaviour has been shown in previous study using potato starch with WI of 28.34 [16]. The yellow index (YI) is found to be significantly higher in the chitosan films and in the blend (CH/ST), which is inherent to the colour of the chitosan used.

With the incorporation of TiO_2 into the blends, the bionanocomposites appear whiter due to the inherent whiteness of the powdered TiO_2 nanoparticles. Therefore, L, ΔE, and WI values are

found to vary between 32.47-45.03, 33.60-45.14, and 30.47-43.17, respectively, which are higher than those of CH/ST blends. The addition of 1% of TiO_2 to the biopolymer blend (CH/ST/T1%) results in a reduction of 57% in the yellow index (YI) and an increase of 38%, 34%, and 41% in the values of L, ΔE, and WI, respectively. Similar behaviour was observed in a previous study for the addition of TiO_2 into Iberian Lallemantia mucilage and potato starch films [16,18]. The measurement data from the colorimeter (Table 2) are in agreement with the photographs of the samples (Fig. 8).

3.8. Opacity and transmittance

Figure 9 shows the UV-vis absorbance spectra in the wavelength ranges of 200–800 nm for films of CH, ST, CH/ST, CH/ST/T0.25%, and CH/ST/T1%. There is a large difference between the absorption of biopolymer films without TiO_2 and that of bionanocomposites with TiO_2 across a wide range of UV and visible regions (Figure 9). The addition of TiO_2 results in a strong increase in absorbance, particularly in the UV region of 200–400 nm. This is similar to what has been previously observed when incorporating TiO_2 in wheat starch films [17]. The strong absorption in the UV region can be attributed to the TiO_2 content, which is a semiconductor with a direct wide bandgap of ~3.05 eV for anatase [25,27]. Biopolymer films without TiO_2 showed a lower absorbance in the UV and visible regions, except for the ST film, which shows a strong broadband absorbance in the region of 240–800nm. This suggests that film opacity is another determining factor that leads to higher absorption and consequently lower transmittance (Table 3). This is evident when comparing the photographs of the films (Figure 8) with the measurement data in Table 3.

Films with TiO_2 nanoparticles demonstrate a significantly lower ($p < 0.05$) transmittance (%T) in UV-A (360 nm), UV-B (300 nm), UV-C (240 nm), and visible regions (600 nm) (Table 3). In comparison to CH/ST films, the bionanocomposite CH/ST/T1% films that contain 1% of TiO_2 exhibit a lower transmittance of >97% in the UVA, UVB, and UVC, as well as >60% in the visible region. This is in agreement with previous studies that show an increase in absorbance of carboxymethylcellulose, gelatin, and potato starch films with the increase of TiO_2 nanoparticles concentration [16,26,44].

The opacity data presented in Table 3 strongly suggests that cassava starch and TiO_2 are the most decisive factors in increasing the opacity of the films. ST films exhibit a significantly greater opacity ($p < 0.05$) than CH and CH/ST blend films. The addition of TiO_2 to the CH/ST blend leads to a significant increase ($p < 0.05$) in opacity compared to the CH/ST without TiO_2. These factors

reflect in the reduction of the transmittance of the films due to the scattering from cassava starch dispersion and the absorption band of the TiO_2 nanoparticles [40,55]. These results suggest that bionanocomposite films made of chitosan and cassava starch blends with the addition of 1% TiO_2 nanoparticles provide good optical properties with the potential to provide prevention against damage induced by UV light.

4. Conclusion

Ecofriendly bioplastics consisting of chitosan/cassava starch/TiO_2 were developed and the results demonstrated that the properties of the films were strongly influenced by the properties of the constituent biopolymers and the concentration of the incorporated TiO_2 nanoparticles. Blend formulation leads to a decrease in water vapour permeability in comparison to chitosan films and a reduction in solubility in relation to cassava starch films with intermediate values for tension, greater elongation, and less water sorption. The incorporation of TiO_2 nanoparticles within the chitosan-cassava starch biofilms provides an opportunity to advance the fundamental understanding of the functional properties of bionanocomposite films. The increase in TiO_2 nanoparticles concentration of up to 1% w/w within the biopolymeric blend resulted in a more hydrophobic film with improved mechanical properties along with water solubility and vapour permeability. The addition of 1% TiO2 in the film also leads to a reduction in light transmittance in the UV regions, thus showing a potential as UV light blocking agents for use as protective packaging to prevent detrimental effects on food. The chitosan/cassava starch/TiO2-based biopolymeric films developed in this work has the potential to enable the development of more sustainable packaging and contribute to the reduction of impacts caused by conventional plastics to the environment. The systematic approach introduced herein can be extrapolated for further development of functional biodegradable films with photoactive components that produces reactive oxygen species and hydroxyl radicals, which may inactivate microorganisms and deplete ethylene, for replacement of existing synthetic polymers.

Funding sources

Universidade Federal Rural do Semi-Árido (UFERSA) and Conselho Nacional de Desenvolvimento Científico e Tecnológico (CNPq).

Declaration of Competing Interest

The authors declare that there is no conflict of interest regarding the publication of this paper.

CRediT authorship contribution statement

Francisco Leonardo Gomes de Menezes: Conceptualisation, Methodology, Investigation, Formal analysis, Writing -original draft.
Edna Maria Mendes Aroucha: Conceptualisation, Supervision, Writing - review & editing.
Francisco Klebson Gomes dos Santos: Conceptualisation, Supervision, Writing - review & editing.
Ricardo Henrique Lima Leite: Conceptualisation, Writing - review & editing.
Adrianus Indrat Aria: Conceptualisation, Writing - review & editing.

Acknowledgment

The authors would like to thank Universidade Federal Rural do Semi-Arido/UFERSA for supporting the research. A.I.A. acknowledges partial support from Marie Skłodowska-Curie Action (Grant 645725, FRIENDS2).

References

[1] Y. Zhong, P. Godwin, Y. Jin, H. Xiao, Biodegradable polymers and green-based antimicrobial packaging materials: A mini-review, Advanced Industrial and Engineering Polymer Research. 3(1) (2020) 27–35. https://doi.org/10.1016/j.aiepr.2019.11.002.

[2] S. Mangaraj, A. Yadav, L.M. Bal, S.K. Dash, N.K. Mahanti, Application of Biodegradable Polymers in Food Packaging Industry: A Comprehensive Review, Journal of Packaging Technology and Research. 3 (2019) 77–96. https://doi.org/10.1007/s41783-018-0049-y.

[3] V.K. Thakur, S.I. Voicu, Recent advances in cellulose and chitosan based membranes for water purification: A concise review, Carbohydrate Polymers. 146 (2016) 148–165. https://doi.org/10.1016/j.carbpol.2016.03.030.

[4] A. Podshivalov, M. Zakharova, E. Glazacheva, M. Uspenskaya, Gelatin/potato starch edible biocomposite films: Correlation between morphology and physical properties, Carbohydrate Polymers. 157 (2017) 1162–1172. https://doi.org/10.1016/j.carbpol.2016.10.079.

[5] S. Soradech, J. Nunthanid, S. Limmatvapirat, M. Luangtana-anan, Utilization of shellac and gelatin composite film for coating to extend the shelf life of banana, Food Control. 73 (2017) 1310–1317. https://doi.org/10.1016/j.foodcont.2016.10.059.

Journal Pre-proof

[6] N.A. Pattanashetti, G.B. Heggannavar, M.Y. Kariduraganavar, Smart Biopolymers and their Biomedical Applications, Procedia Manufacturing. 12 (2017) 263–279. https://doi.org/10.1016/j.promfg.2017.08.030.

[7] V.R.L. Oliveira, F.K.G. Santos, R.H.L. Leite, E.M.M. Aroucha, K.N.O. Silva, Use of biopolymeric coating hydrophobized with beeswax in post-harvest conservation of guavas, Food Chemistry. 259 (2018) 55–64. https://doi.org/10.1016/j.foodchem.2018.03.101.

[8] B. Ates, S. Koytepe, A. Ulu, C. Gurses, V.K. Thakur, Chemistry, Structures, and Advanced Applications of Nanocomposites from Biorenewable Resources, Chemical Reviews. 120 (2020) 9304–9362. https://doi.org/10.1021/acs.chemrev.9b00553.

[9] C.M. Machado, P. Benelli, I.C. Tessaro, Sesame cake incorporation on cassava starch foams for packaging use, Industrial Crops and Products. 102 (2017) 115–121. https://doi.org/10.1016/j.indcrop.2017.03.007.

[10] R. Balti, M. Ben Mansour, N. Sayari, L. Yacoubi, L. Rabaoui, N. Brodu, A. Massé, Development and characterization of bioactive edible films from spider crab (Maja crispata) chitosan incorporated with Spirulina extract, International Journal of Biological Macromolecules. 105 (2017) 1464–1472. https://doi.org/10.1016/j.ijbiomac.2017.07.046.

[11] E.M. de A. Braz, S.C.C.C. e. Silva, D.A. da Silva, F.A. de A. Carvalho, H.M. Barreto, L. de S. Santos Júnior, E.C. da Silva Filho, Modified chitosan-based bioactive material for antimicrobial application: Synthesis and characterization, International Journal of Biological Macromolecules. 117 (2018) 640–647. https://doi.org/10.1016/j.ijbiomac.2018.05.205.

[12] S. Gopi, A. Amalraj, S. Jude, S. Thomas, Q. Guo, Bionanocomposite films based on potato, tapioca starch and chitosan reinforced with cellulose nanofiber isolated from turmeric spent, Journal of the Taiwan Institute of Chemical Engineers. 96 (2019) 664–671. https://doi.org/10.1016/j.jtice.2019.01.003.

[13] H. Wang, J. Qian, F. Ding, Emerging Chitosan-Based Films for Food Packaging Applications, Journal of Agricultural and Food Chemistry. 66(2) (2018) 395–413. https://doi.org/10.1021/acs.jafc.7b04528.

[14] B. Zhang, J.Q. Mei, B. Chen, H.Q. Chen, Digestibility, physicochemical and structural properties of octenyl succinic anhydride-modified cassava starches with different degree of substitution, Food Chemistry. 229 (2017) 136–141. https://doi.org/10.1016/j.foodchem.2017.02.061.

[15] J. Colivet, R.A. Carvalho, Hydrophilicity and physicochemical properties of chemically modified cassava starch films, Industrial Crops and Products. 95 (2017) 599–607. https://doi.org/10.1016/j.indcrop.2016.11.018.

[16] S.A. Oleyaei, Y. Zahedi, B. Ghanbarzadeh, A.A. Moayedi, Modification of physicochemical and thermal properties of starch films by incorporation of TiO_2 nanoparticles, International Journal of Biological Macromolecules. 89 (2016) 256–264. https://doi.org/10.1016/j.ijbiomac.2016.04.078.

[17] V. Goudarzi, I. Shahabi-Ghahfarrokhi, A. Babaei-Ghazvini, Preparation of ecofriendly UV-protective food packaging material by starch/TiO_2 bio-nanocomposite: Characterization,

International Journal of Biological Macromolecules. 95 (2017) 306–313. https://doi.org/10.1016/j.ijbiomac.2016.11.065.

[18] A. Sadeghi-Varkani, Z. Emam-Djomeh, G. Askari, Morphology and physicochemical properties of a novel Lallemantia iberica mucilage/titanium dioxide bio-nanocomposite, Polymer Testing. 67 (2018) 12–21. https://doi.org/10.1016/j.polymertesting.2018.02.006.

[19] U. Siripatrawan, P. Kaewklin, Fabrication and characterization of chitosan-titanium dioxide nanocomposite film as ethylene scavenging and antimicrobial active food packaging, Food Hydrocolloids. 84 (2018) 125–134. https://doi.org/10.1016/j.foodhyd.2018.04.049.

[20] L. Qu, G. Chen, S. Dong, Y. Huo, Z. Yin, S. Li, Y. Chen, Improved mechanical and antimicrobial properties of zein/chitosan films by adding highly dispersed nano-TiO_2, Industrial Crops and Products. 130 (2019) 450–458. https://doi.org/10.1016/j.indcrop.2018.12.093.

[21] J. de M. Fonseca, G.A. Valencia, L.S. Soares, M.E.R. Dotto, C.E.M. Campos, R. de F.P.M. Moreira, A.R.M. Fritz, Hydroxypropyl methylcellulose-TiO_2 and gelatin-TiO_2 nanocomposite films: Physicochemical and structural properties, International Journal of Biological Macromolecules. 151 (2020) 944–956. https://doi.org/10.1016/j.ijbiomac.2019.11.082.

[22] P. Kaewklin, U. Siripatrawan, A. Suwanagul, Y.S. Lee, Active packaging from chitosan-titanium dioxide nanocomposite film for prolonging storage life of tomato fruit, International Journal of Biological Macromolecules. 112 (2018) 523–529. https://doi.org/10.1016/j.ijbiomac.2018.01.124.

[23] Y. Xing, H. Yang, X. Guo, X. Bi, X. Liu, Q. Xu, Q. Wang, W. Li, X. Li, Y. Shui, C. Chen, Y. Zheng, Effect of chitosan/Nano-TiO_2 composite coatings on the postharvest quality and physicochemical characteristics of mango fruits, Scientia Horticulturae. 263 (2020) 109135. https://doi.org/10.1016/j.scienta.2019.109135.

[24] J. González-Benito, J. Teno, G. González-Gaitano, S. Xu, M.Y. Chiang, PVDF/TiO_2 nanocomposites prepared by solution blow spinning: Surface properties and their relation with S. Mutans adhesion, Polymer Testing. 58 (2017) 21–30. https://doi.org/10.1016/j.polymertesting.2016.12.005.

[25] M. Hoseinnejad, S. Mahdi Jafari, I. Katouzian, Inorganic and metal nanoparticles and their antimicrobial activity in food packaging applications, Critical Reviews in Microbiology. 44(2) (2018) 161–181. https://doi.org/10.1080/1040841x.2017.1332001.

[26] B. Fathi Achachlouei, Y. Zahedi, Fabrication and characterization of CMC-based nanocomposites reinforced with sodium montmorillonite and TiO_2 nanomaterials, Carbohydrate Polymers. 199 (2018) 415–425. https://doi.org/10.1016/j.carbpol.2018.07.031.

[27] Z. Zhu, H. Cai, D.W. Sun, Titanium dioxide (TiO_2) photocatalysis technology for nonthermal inactivation of microorganisms in foods, Trends in Food Science & Technology. 75 (2018) 23–35. https://doi.org/10.1016/j.tifs.2018.02.018.

[28] V. Goudarzi, I. Shahabi-Ghahfarrokhi, Development of photo-modified starch/kefiran/TiO_2 bio-nanocomposite as an environmentally-friendly food packaging material, International

Journal of Biological Macromolecules. 116 (2018) 1082–1088. https://doi.org/10.1016/j.ijbiomac.2018.05.138.

[29] K. Rambabu, G. Bharath, F. Banat, P.L. Show, H.H. Cocoletzi, Mango leaf extract incorporated chitosan antioxidant film for active food packaging, International Journal of Biological Macromolecules. 126 (2019) 1234–1243. https://doi.org/10.1016/j.ijbiomac.2018.12.196.

[30] M. Alizadeh-Sani, J.W. Rhim, M. Azizi-Lalabadi, M. Hemmati-Dinarvand, A. Ehsani, Preparation and characterization of functional sodium caseinate/guar gum/TiO_2/cumin essential oil composite film, International Journal of Biological Macromolecules. 145 (2020) 835–844. https://doi.org/10.1016/j.ijbiomac.2019.11.004.

[31] F. Loosli, S. Stoll, Effect of surfactants, pH and water hardness on the surface properties and agglomeration behavior of engineered TiO_2 nanoparticles, Environmental Science Nano. 4 (2017) 203–211. https://doi.org/10.1039/c6en00339g.

[32] C. Guiot, O. Spalla, Stabilization of TiO_2 Nanoparticles in Complex Medium through a pH Adjustment Protocol, Environmental Science & Technology. 47 (2013) 1057–1064. https://doi.org/10.1021/es3040736.

[33] N.T.K. Thanh, N. Maclean, S. Mahiddine, Mechanisms of Nucleation and Growth of Nanoparticles in Solution, Chemical Reviews. 114 (2014) 7610–7630. https://doi.org/10.1021/cr400544s.

[34] L. Luo, P. Wang, D. Jing, X. Wang, Self-assembly of TiO2 nanoparticles into chains, films and honeycomb networks, CrystEngComm. 16 (2014) 1584–1591. https://doi.org/10.1039/c3ce41709c.

[35] F.A. Al-Sagheer, S. Merchant, Visco-elastic properties of chitosan–titania nano-composites, Carbohydrate Polymers. 85(2) (2011) 356–362. https://doi.org/10.1016/j.carbpol.2011.02.032.

[36] J. Polte, Fundamental growth principles of colloidal metal nanoparticles – a new perspective, CrystEngComm. 17 (2015) 6809–6830. https://doi.org/10.1039/C5CE01014D.

[37] B. Li, Y. Zhang, Y. Yang, W. Qiu, X. Wang, B. Liu, Y. Wang, G. Sun, Synthesis, characterization, and antibacterial activity of chitosan/TiO_2 nanocomposite against Xanthomonas oryzae pv. oryzae, Carbohydrate Polymers. 152 (2016) 825–831. https://doi.org/10.1016/j.carbpol.2016.07.070.

[38] B. Lin, Y. Luo, Z. Teng, B. Zhang, B. Zhou, Q. Wang, Development of silver/titanium dioxide/chitosan adipate nanocomposite as an antibacterial coating for fruit storage, LWT - Food Science and Technology. 63 (2015) 1206–1213. https://doi.org/10.1016/j.lwt.2015.04.049.

[39] Y. Zhang, C. Xue, Y. Xue, R. Gao, X. Zhang, Determination of the degree of deacetylation of chitin and chitosan by X-ray powder diffraction, Carbohydrate Research. 340 (2005) 1914–1917. https://doi.org/10.1016/j.carres.2005.05.005.

[40] Y. Li, Y. Jiang, F. Liu, F. Ren, G. Zhao, X. Leng, Fabrication and characterization of

Journal Pre-proof

TiO_2/whey protein isolate nanocomposite film, Food Hydrocolloids. 25(5) (2011) 1098–1104. https://doi.org/10.1016/j.foodhyd.2010.10.006.

[41] P. Cazón, M. Vázquez, Mechanical and barrier properties of chitosan combined with other components as food packaging film, Environmental Chemistry Letters. 18(2) (2020) 257–267. https://doi.org/10.1007/s10311-019-00936-3.

[42] S. Santacruz, C. Rivadeneira, M. Castro, Edible films based on starch and chitosan. Effect of starch source and concentration, plasticizer, surfactant's hydrophobic tail and mechanical treatment, Food Hydrocolloids. 49 (2015) 89–94. https://doi.org/10.1016/j.foodhyd.2015.03.019.

[43] M. Zolfi, F. Khodaiyan, M. Mousavi, M. Hashemi, Development and characterization of the kefiran-whey protein isolate-TiO_2 nanocomposite films, International Journal of Biological Macromolecules. 65 (2014) 340–345. https://doi.org/10.1016/j.ijbiomac.2014.01.010.

[44] Q. He, Y. Zhang, X. Cai, S. Wang, Fabrication of gelatin–TiO_2 nanocomposite film and its structural, antibacterial and physical properties, International Journal of Biological Macromolecules. 84 (2016) 153–160. https://doi.org/10.1016/j.ijbiomac.2015.12.012.

[45] J.J. Zhou, S.Y. Wang, S. Gunasekaran, Preparation and Characterization of Whey Protein Film Incorporated with TiO_2 Nanoparticles, Journal of Food Science. 74(7) (2009) 50–56. https://doi.org/10.1111/j.1750-3841.2009.01270.x.

[46] A. Zomorodian, Z. Kavoosi, L. Momenzadeh, Determination of EMC isotherms and appropriate mathematical models for canola, Food and Bioproducts Processing. 89(4) (2011) 407–413. https://doi.org/10.1016/j.fbp.2010.10.006.

[47] G. Ghayal, A. Jha, J.K. Sahu, A. Kumar, A. Gautam, R. Kumar, P. Rasane, Moisture sorption isotherms of dietetic Rabri at different storage temperatures, International Journal of Dairy Technology. 66(4) (2013) 587–594. https://doi.org/10.1111/1471-0307.12083.

[48] A. Mohammadi Nafchi, M. Moradpour, M. Saeidi, A.K. Alias, Effects of nanorod-rich ZnO on rheological, sorption isotherm, and physicochemical properties of bovine gelatin films, LWT-Food Science and Technology. 58(1) (2014) 142–149. https://doi.org/10.1016/j.lwt.2014.03.007.

[49] W. Zhang, J. Chen, Y. Chen, W. Xia, Y.L. Xiong, H. Wang, Enhanced physicochemical properties of chitosan/whey protein isolate composite film by sodium laurate-modified TiO_2 nanoparticles, Carbohydrate Polymers. 138 (2016) 59–65. https://doi.org/10.1016/j.carbpol.2015.11.031.

[50] M.L. Monte, M.L. Moreno, J. Senna, L.S. Arrieche, L.A.A. Pinto, Moisture sorption isotherms of chitosan-glycerol films: Thermodynamic properties and microstructure, Food Bioscience. 22 (2018) 170–177. https://doi.org/10.1016/j.fbio.2018.02.004.

[51] B.R.B. Lara, M.V. Dias, M. Guimarães Junior, P.S. de Andrade, B. de Souza Nascimento, L.F. Ferreira, M.I. Yoshida, Water sorption thermodynamic behavior of whey protein isolate/ polyvinyl alcohol blends for food packaging, Food Hydrocolloids. 103 (2020) 105710. https://doi.org/10.1016/j.foodhyd.2020.105710.

Journal Pre-proof

[52] M.D. Torres, R. Moreira, F. Chenlo, M.J. Vázquez, Water adsorption isotherms of carboxymethyl cellulose, guar, locust bean, tragacanth and xanthan gums, Carbohydrate Polymers. 89(2) (2012) 592–598. https://doi.org/10.1016/j.carbpol.2012.03.055.

[53] F. Debiagi, Beatriz, M. Marim, S. Mali, Properties of Cassava Bagasse and Polyvinyl Alcohol Biodegradable Foams, Journal of Polymers and the Environment. 23(2) (2015) 269–276. https://doi.org/10.1007/s10924-014-0705-4.

[54] J.I. Enrione, S.E. Hill, J.R. Mitchell, Sorption Behavior of Mixtures of Glycerol and Starch, Journal of Agricultural and Food Chemistry. 55(8) (2007) 2956–2963. https://doi.org/10.1021/jf062186c.

[55] T. Smijs, Pavel, Titanium dioxide and zinc oxide nanoparticles in sunscreens: focus on their safety and effectiveness, Nanotechnology, Science and Applications. 4 (2011) 95-112. https://doi.org/10.2147/nsa.S19419.

Figure legends

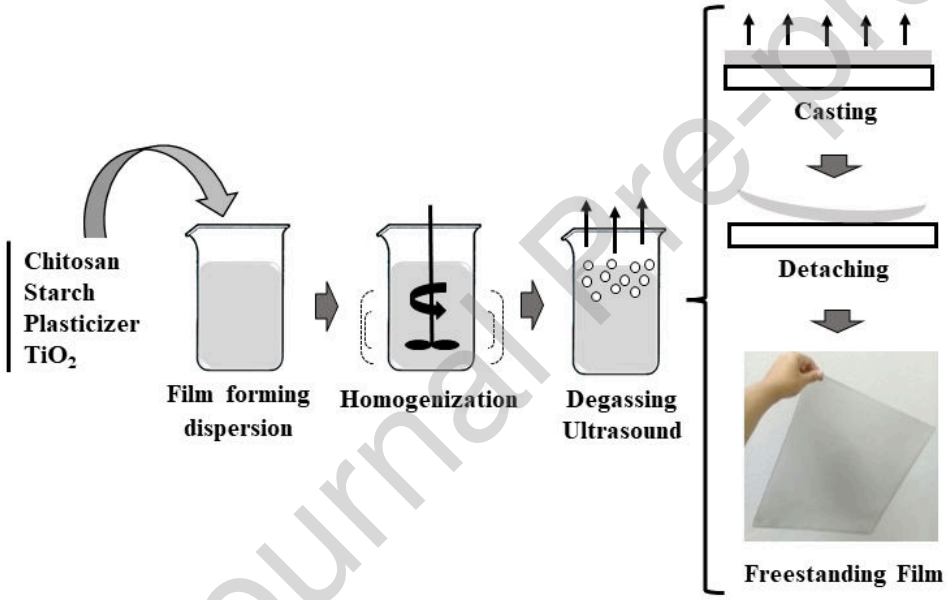


Figure 1. Schematic representation of the preparation of films CH, ST, CH/ST, CH/ST/T 0.25% and CH/ST/T 1%.

Journal Pre-proof

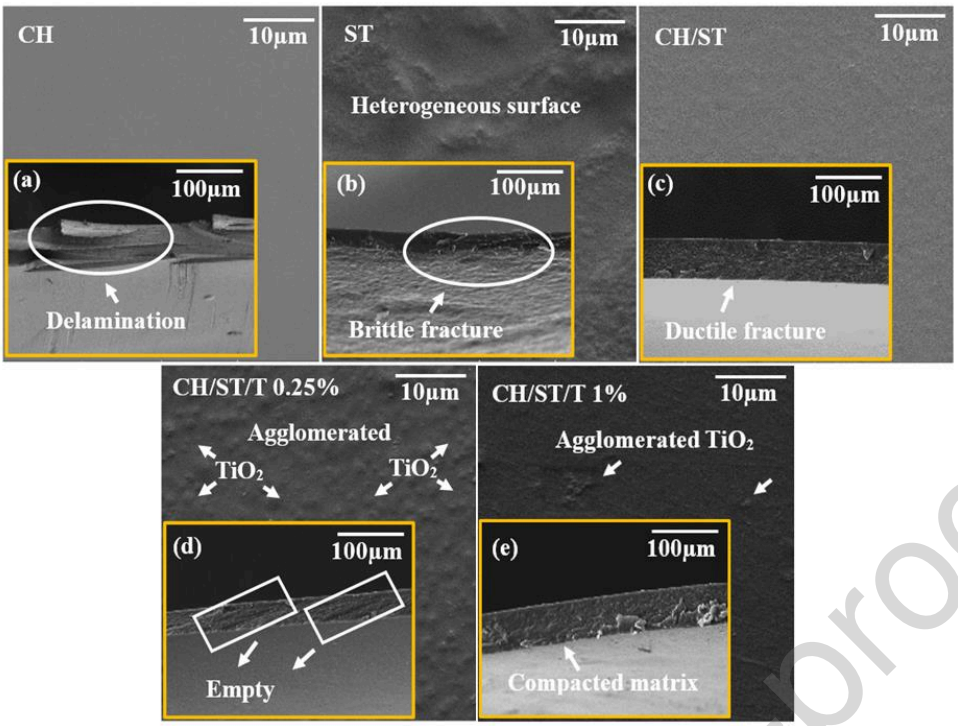


Figure 2. SEM images of the surface and the cross-section (insets) of the biofilms (top left to right: CH, ST, and CH/ST) and bionanocomposites (bottom left to right: CH/ST/T0.25% and CH/ST/T1%).

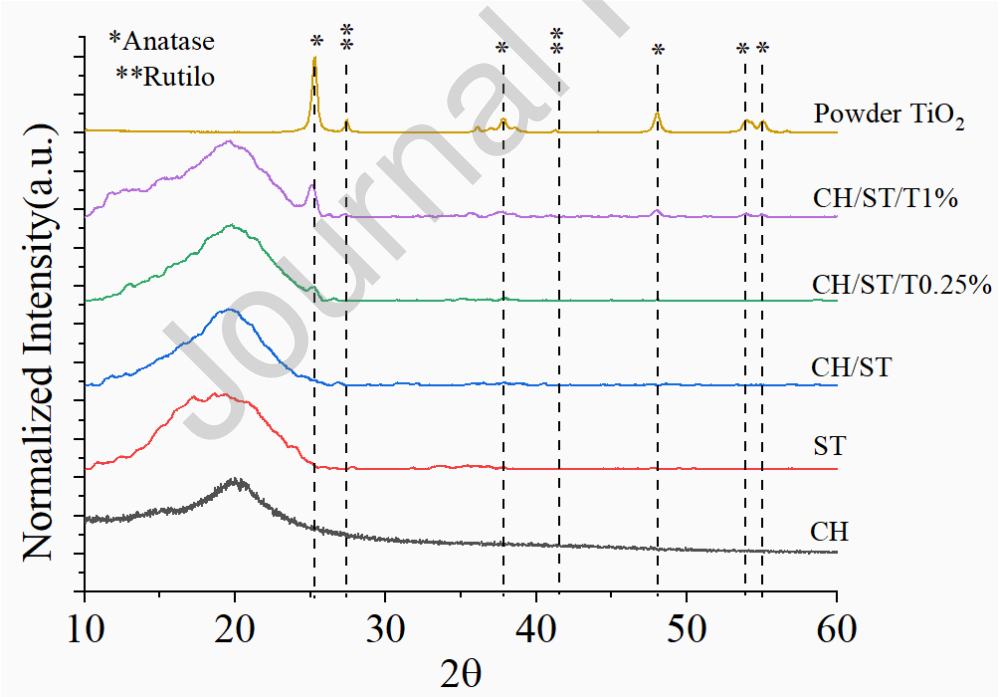


Figure 3. X-ray diffraction patterns of CH, ST, CH/ST, CH/ST/T0.25%, and CH/ST/T1% films with that of TiO_2 nanoparticles powder as a comparison. The powdered TiO_2 nanoparticles exhibit 2θ diffraction peaks correspond to anatase phase (*) at 25°, 37.5º, 48º, 54 ° and 55º, and to rutile phase (**) at 27° and 42º.

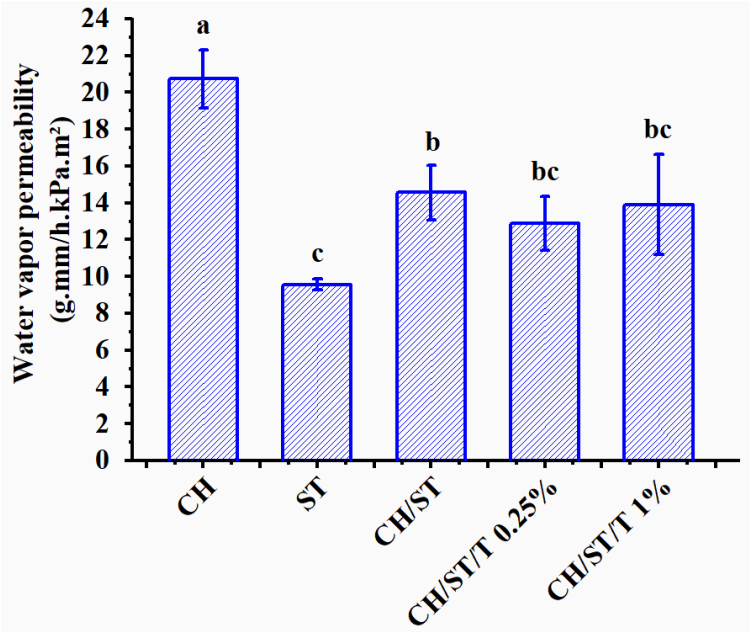


Figure 4. Water vapour permeability of CH, ST, CH/ST, CH/ST/T0.25%, and CH/ST/T1%. Different letters indicate statistical difference ($p < 0.05$). Vertical error bars indicate the standard deviation (SD) from the mean with n = 5.

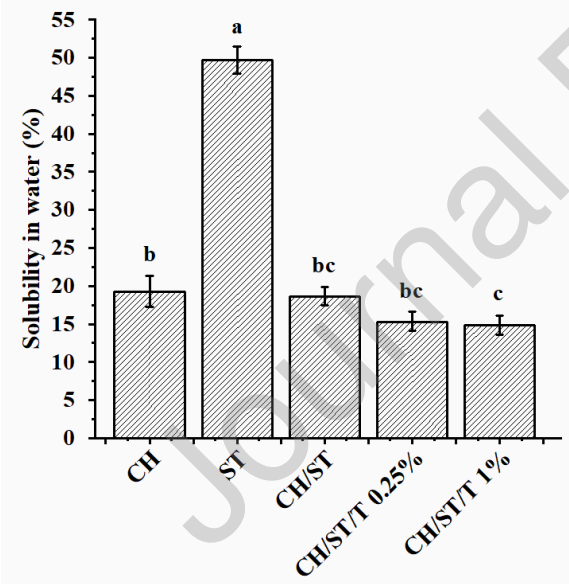


Figure 5. Water solubility of CH, ST, CH/ST, CH/ST/T0.25% and CH/ST/T1%. Different letters indicate statistical difference ($p < 0.05$). Vertical error bars indicate the standard deviation (SD) from the mean with n = 5.

Journal Pre-proof

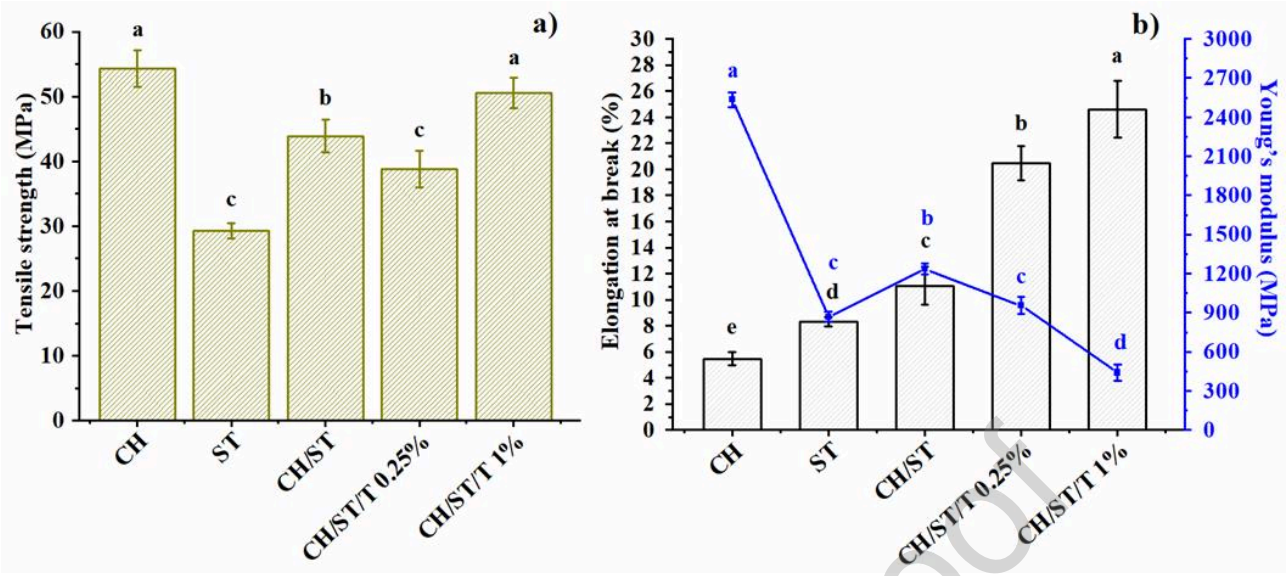


Figure 6. Mechanical properties: (a) Tensile strength, (b) elongation at break, and Young's modulus of CH, ST, CH/ST, CH/ST/T0.25%, and CH/ST/T1%. Different letters indicate statistical difference ($p < 0.05$). Vertical error bars indicate the standard deviation (SD) from the mean with n =5.

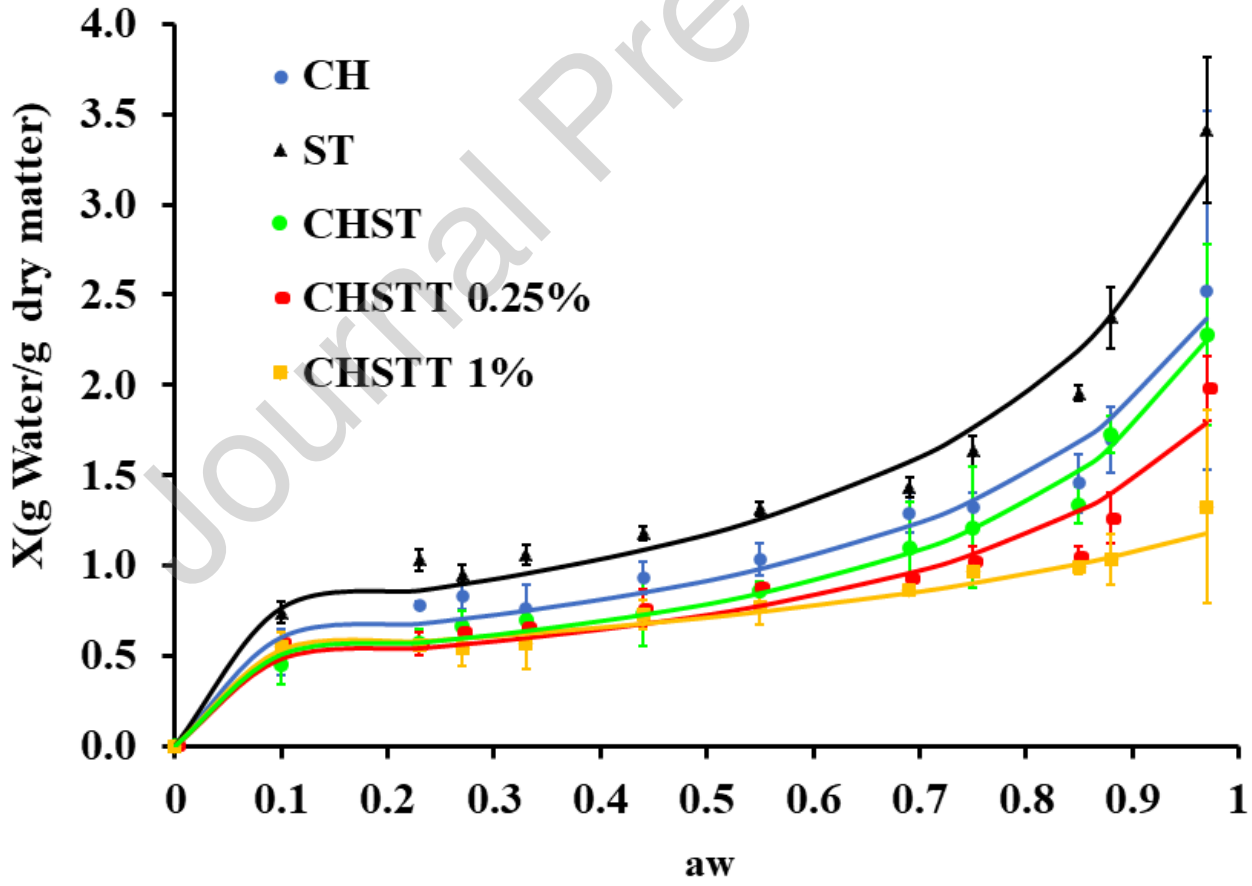


Figure 7. Water sorption isotherms for CH, ST, CH/ST, CH/ST/T0.25% and CH/ST/T1% films at 25 °C. Data points and lines represent experimental observation and GAB model fittings,

respectively. Water sorption is presented as the amount of water per dry matter (X) as a function of water activity (a_w). Vertical error bars indicate the standard deviation (SD). n =5.

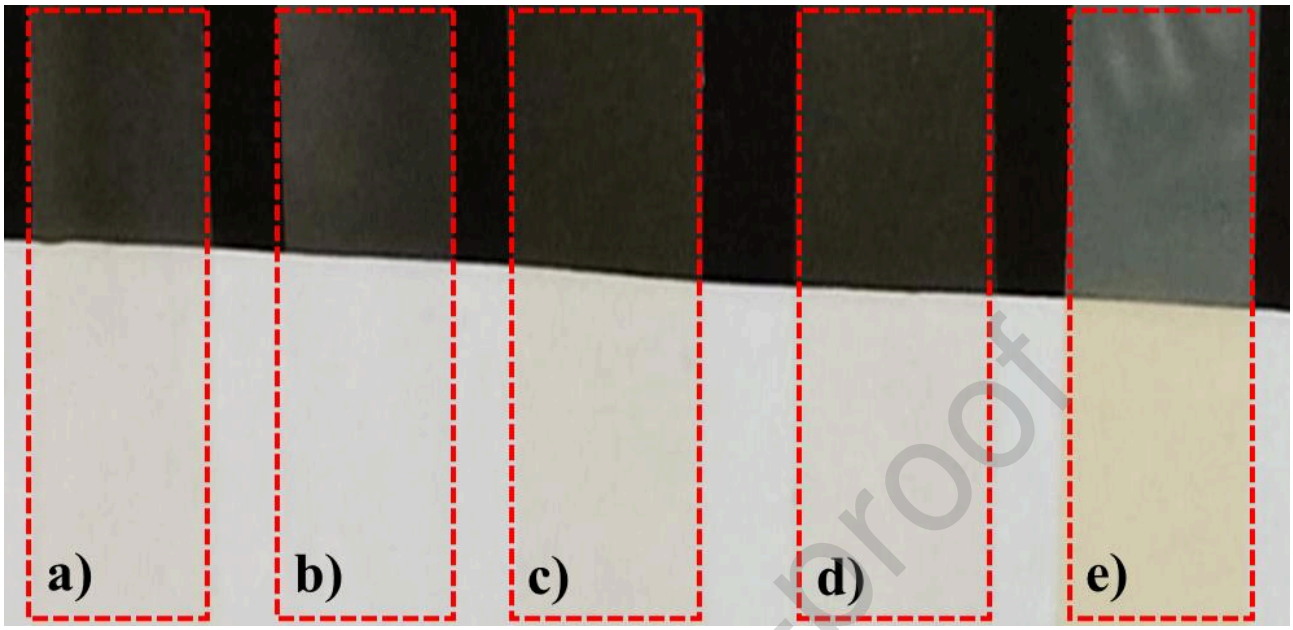


Figure 8. Photo taken of films a) CH, b) ST, c) CH/ST, d) CH/ST/T 0.25% and e) CH/ST/T 1%) on a standard black and white background.

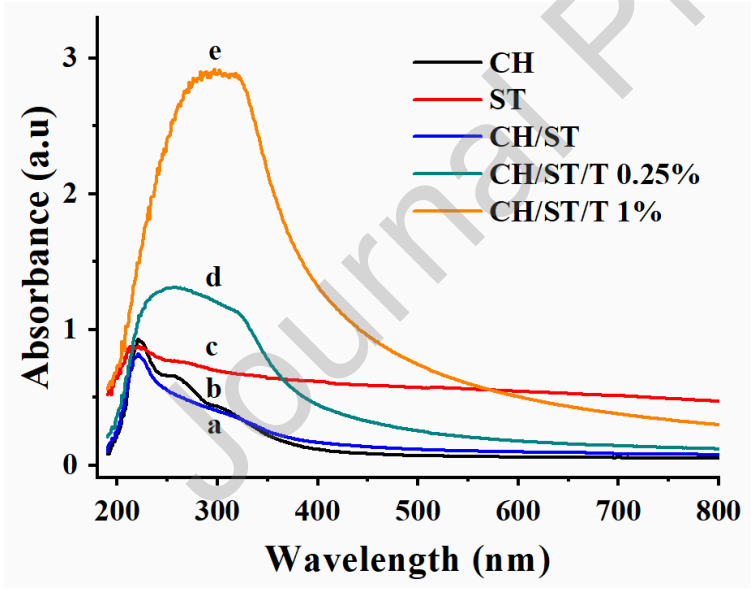


Figure 9. UV-vis absorbance spectra of films (a) CH, (b) ST, (c) CH/ST, (d) CH/ST/T0.25%, and (e) CH/ST/T1%.

Journal Pre-proof

Table legends

Table 1. GAB parameters for the moisture sorption isotherms of CH, ST, CH/ST, CH/ST/T0.25% and CH/ST/T1% films at 25 °C.

Film	Model Constants GAB (a_w = 0.11-0.96)				
	x_m (g water/g dry solid)	C	K	R^2	$R^2_{adjusted}$
CH	0.5565	$5.59x10^5$	0.7887	0.9684	0.9613
ST	0.7047	$6.07x10^7$	0.8009	0.9799	0.9755
CH/ST	0,4662	$5.59x10^5$	0.8169	0.9870	0.9841
CH/ST/T 0.25%	0.4470	$2.44x10^6$	0,7735	0,9378	0.9240
CH/ST/T 1%	0.5010	$1.52x10^{11}$	0.5914	0.9700	0.9633

Table 2. Thickness and colour parameters of CH, ST, CH/ST, CH/ST/T 025% and CH/ST/T1% films. Dataset is presented as mean ± standard deviation. Different letters indicate statistical difference ($p < 0.05$).

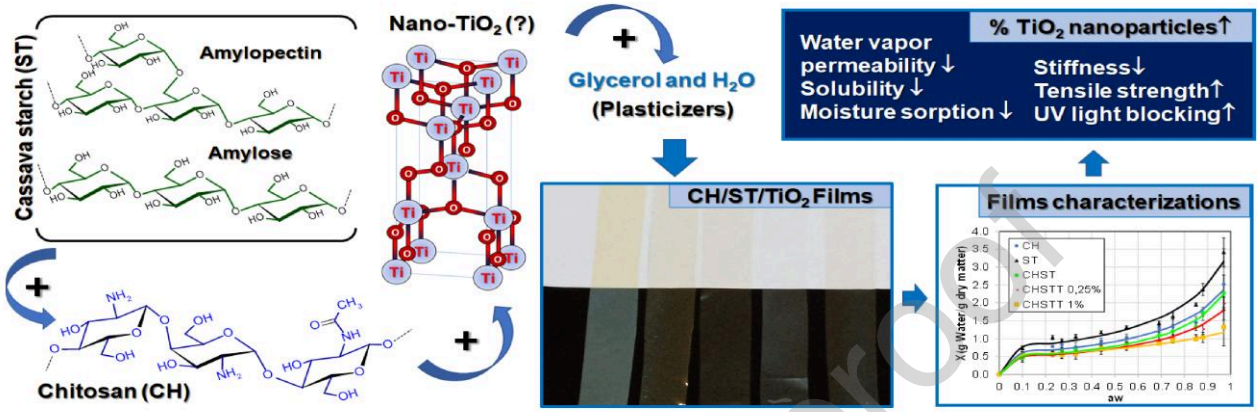
Film	Thickness (mm)	L	ΔE	WI	YI
CH	0.07 ± 0.01a	36.53 ± 0.06b	37.96 ± 0.12b	34.17 ± 0.04b	49.72 ± 0.21a
ST	0.04 ± 0.01b	32.17 ± 0.06d	33.22 ± 0.03d	30.23 ± 0.12c	47.36 ± 0.23b
CH/ST	0.06 ± 0.01ab	32.47 ± 0.06d	33.60 ± 0.08d	30.47 ± 0.06c	48.88 ± 0.48a
CH/ST/T0.25%	0.05 ± 0.01ab	35.87 ± 0.35c	36.47 ± 0.35c	34.00 ± 0.30b	37.56 ± 0.59c
CH/ST/T1%	0.05 ± 0.01ab	45.03 ± 0.38a	45.14 ± 0.42a	43.17 ± 0.32a	20.87 ± 0.70d

Table 3. Opacity and transmittance of films in the UV-C, UV-B, UV-A, and visible regions. Dataset is presented as mean ± standard deviation. Different letters indicate statistical difference ($p < 0.05$).

Film	UVC (240 nm) T (%)	UVB (300 nm) T (%)	UVA (360 nm) T (%)	Visible (600 nm) T (%)	Opacity (AU.Nm/mm)
CH	20.51 ± 0.83b	36.98 ± 1.25a	64.42 ± 0.88a	87.15 ± 0.50a	0.79 ± 0.03e
ST	15.93 ± 0.38c	19.86 ± 1.05b	22.72 ± 1.22c	27.99 ± 1.90e	13.50 ± 0.70a
CH/ST	23.21 ± 2.36a	38.48 ± 2.59a	58.51 ± 2.10b	79.49 ± 0.95b	1.75 ± 0.09d
CH/ST/T0.25%	5.53 ± 0.25d	6.64 ± 0.40c	21.29 ± 1.30c	66.10 ± 2.48c	4.09 ± 0.36c

CH/ST/T1%	0.69 ± 0.17e	0.14 ± 0.07d	1.30 ± 0.36d	31.76 ± 1.58d	9.97 ± 0.42b

Graphical abstract



Journal Pre-proof

CRediT authorship contribution statement

Francisco Leonardo Gomes de Menezes: Conceptualisation, Methodology, Investigation, Formal analysis, Writing -original draft.
Edna Maria Mendes Aroucha: Conceptualisation, Supervision, Writing - review & editing.
Francisco Klebson Gomes dos Santos: Conceptualisation, Supervision, Writing - review & editing.
Ricardo Henrique Lima Leite: Conceptualisation, Writing - review & editing.
Adrianus Indrat Aria: Conceptualisation, Writing - review & editing.

Journal Pre-proof

Declaration of interests

☒The authors declare that they have no known competing financial interests or personal relationships that could have appeared to influence the work reported in this paper.

☐The authors declare the following financial interests/personal relationships which may be considered as potential competing interests:

Journal Pre-proof

Highlights

- Ecofriendly material based on chitosan, cassava starch and TiO_2 was developed.
- Hygroscopicity and stiffness were reduced in biopolymers blends based films.
- Water vapor permeability and solubility decreased with TiO_2 nanoparticles addition.
- The nanoparticles improved mechanical properties of the films.
- TiO_2 led to a reduction in transmittance of more than 97% in UV regions.

Journal Pre-proof



https://dspace.org/

TiO2-enhanced chitosan/cassava starch biofilms for sustainable food packaging

Gomes de Menezes, Francisco Leonardo; Henriquede Lima Leite, Ricardo; Gomes dos Santos, Francisco Klebson; Aria, Adrianus Indrat; Mendes Aroucha, Edna Maria

2021-10-01
Elsevier
https://doi.org/10.1016/j.colsurfa.2021.127661
Gomes de Menezes FL, Henrique de Lima Leite R, Gomes dos Santos FK, et al., (2021) TiO2-enhanced chitosan/cassava starch biofilms for sustainable food packaging. Colloids and Surfaces A: Physicochemical and Engineering Aspects, Volume 630, December 2021, Article number 127661

Downloaded from a DSpace repository. https://dspace.org/